Experimental investigation of CNT effect on curved beam strength and interlaminar fracture toughness of CFRP laminates

M A Arca[12], **D Coker**[34]
[1] M.Sc., Dept. of Aerospace Engineering, METU, 06800 Ankara, Turkey
[2] Research Assistant, Dept. of Aerospace Engineering, METU 06800 Ankara, Turkey
[3] Assoc. Prof., Dept. of Aerospace Engineering, METU, 06800 Ankara, Turkey
[4] Assoc. Prof., METU Center for Wind Energy (METUWIND), 06800 Ankara, Turkey

E-mail: mirayarca@gmail.com
E-mail: coker@metu.edu.tr

Abstract. High mechanical properties and light weight structures of composite materials and advances in manufacturing processes have increased the use of composite materials in the aerospace and wind energy industries as a primary load carrying structures in complex shapes. However, use of composite materials in complex geometries such as L-shaped laminates creates weakness at the radius which causes delamination. Carbon nanotubes (CNTs) is preferred as a toughening materials in composite matrices due to their high mechanical properties and aspect ratios. However, effect of CNTs on curved beam strength (CBS) is not investigated in literature comprehensively. The objective of this study is to investigate the effect of CNT on Mode I and Mode II fracture toughness and CBS. L-shaped beams are fabric carbon/epoxy composite laminates manufactured by hand layup technique. Curved beam composite laminates were subjected to four point bending loading according to ASTM D6415/D6415M–06a. Double cantilever beam (DCB) tests and end notch flexure (ENF) tests were conducted to determine mode-I and mode-II fracture toughness, respectively. Preliminary results show that 3% CNT addition to the resin increased the mode-I fracture toughness by %25 and mode-II fracture toughness by %10 compared to base laminates. In contrast, no effect on curved beam strength was found.

1. Introduction

Composite material demand in aerospace and wind energy industries is flourishing as a primary load carrying members in complex shapes. However, use of composites in complex geometries such as curved composite beams is problematic for load carrying applications due to their weakness at the radius. Material response and fracture behavior of composites are different from the metallic parts due to the anisotropic behavior of composites. The weakness is caused by high opening stresses at the curved region between the layers leading delamination with loss of toughness. Carbon nanotubes (CNTs) as a toughening material in composite matrix have attracted attention due to their very high mechanical properties and aspect ratios. However, superior properties of CNTs have not been yet realized in the fracture of composites. In the study of Avalon and Donaldson (2010) 5 wt % carbon nanofiber addition to the resin was found to have no overall effect on curved beam strength (CBS) except changing the failure mode from rapid load drop to stick slip behavior and the radial stress at failure was found to be

independent of any parameters (radius, thickness, CNT) for all configurations in both experimental and computational studies, [1]. Yao et al. (2012) investigated CBS and deformation field of curved laminates with different thickness and radius under bending by Digital Speckle Correlation Method and strain gages. Delamination initiation and propagation between 0/0 layers where maximum strain occurs before fracture and unstable to stable failure change with increasing thickness were observed [2]. In their study Seyhan, Tanoglu and Schulte (2008) found that 0.1% wt CNT addition to the resin of E-glass fabric composites increased G_{IIC} by 8% and ILSS by 11%, however it has no effect on G_{IC}, only steady state of R curve was found to decrease. [3]. Godara et al (2009) investigated mechanical properties and Mode I fracture toughness change of different type of 0.5 % wt CNT added [0] prepreg composite laminates. 80% increase in Mode I fracture toughness was observed, however no significant effect on modulus, strength and ILSS was found. Thin multi-walled carbon nanotube (TMWCNT) and DWCNT decreased the thermal expansion coefficient with respect to base materials and CNT bridging was observed [4]. In Garcia, Wardle and Hart's study (2008) DCB and ENF tests were conducted with two unidirectional prepregs having vertically aligned CNTs with different lengths in different plies. A 2 fold and 3 fold improvement of G_{IC} and G_{IIC} respectively was observed [5]. Arai et al. investigated the effect of multi-walled carbon nanotube (MWCNT) and vapor grown carbon fiber (VGCF) interlayer and interlayer thickness on the mode-I and mode-II fracture toughness. They showed that there is an optimum interlayer thickness increasing both G_{IC} and G_{IIC} nearly two times and an increase of 50%in G_{IC} for all interlayer thicknesses [6].

The objective of this study is to experimentally investigate the effect of CNT addition on curved beam strength and on Mode I and Mode II fracture toughness. The curved beams are plain weave fabric carbon/epoxy composite laminates manufactured by hand layup technique with 3 wt % CNT fractions in the resin. High speed cameras in conjunction with digital image correlation method is used in order to obtain deformation field and maximum stress locations and failure sequences. Load displacement curves, high speed camera photos, DIC pictures of maximum stress locations and pictures of fracture surfaces are discussed.

2. Material

Tests are conducted on [0/90] fabric laminate with and without CNT reinforcement. Base material is HexPly® AS4 family 5HS plain weave [0/90] carbon fabric/epoxy prepregs having 0.25 mm ply thickness. CNT added specimens are made of HexPly® AS4 family 5HS plain weave [0/90] carbon dry fabrics having 0.35mm ply thickness. 3% wt CNT addition to the resin is achieved by mixing Araldite® LY 5052 epoxy resin with Epocyl™ NCR128-02 liquid Bisphenol-A epoxy resin (master batch) having high (20 wt %) fraction CNT produced by Nanocyl company in the ratio of 6 to 1 respectively. In the figure 1a CNT bundles and in figure 1b well dispersion of CNTs in the Bisphenol-A epoxy resin can be seen. In the manufacturing process of CNT reinforced laminates the dry fabrics are covered with this CNT-epoxy mix resin.

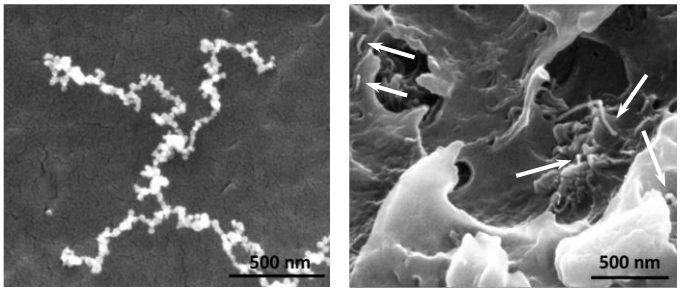

(a) (b)

Figure 1. SEM images of **(a)** CNT bundles compared to **(b)** well dispersed CNTs in the Epocyl™ NCR128-02 liquid Bisphenol-A epoxy resin 20 wt % CNT fraction.

Base and CNT added L-shaped laminates are manufactured by hand layup technique in a right angled male tool using prepregs and dry fabrics, respectively. When the lay-up process was finished, the mold with specimens was wrapped with release film, breather fabric, and vacuum bag, respectively. The length of the legs are 100 mm and 240 mm with the long leg containing a 75 mm Teflon film at the mid

layer to use in fracture toughness tests (DCB and ENF) as shown in Figure 2. Base laminates were made of 12 plies with a thickness of 3 mm. 8 CNT added plies were used in order to obtain 3 mm thick laminates, however after manufacturing thickness of CNT added specimens were measured as 4 mm. Four point bend specimens and fracture toughness tests specimens were obtained by cutting the longer leg of the manufactured specimen 90 mm away from the end of the curved part by using diamond saw cutting machine. Dimensions and geometry of test specimens are given in Table 1 and Figure 2 respectively.

Table 1 Specimen dimensions and number used in each type of tests.

	DCB		ENF		4-pt bending	
	Base	CNT	Base	CNT	Base	CNT
Ply #	12	8	12	8	12	8
Dimensions (mm)	L=135 w=25 t=3	L=135 w=25 t=4	L=135 w=25 t=3	L=135 w=25 t=4	L1=L2=100 w=25 t=3	L1=L2=100 w=25 t=4
# of specimens	2	2	2	2	2	3

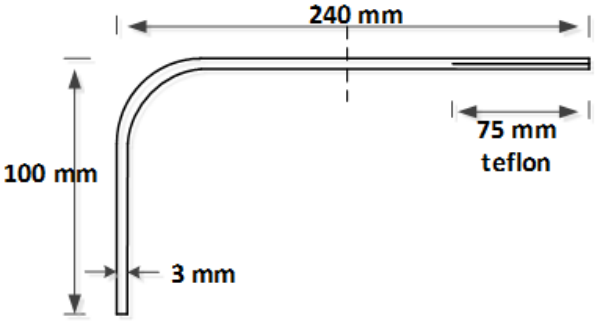

Figure 2. Specimen geometry and dimensions.

3. Experimental Procedure

The Mode I fracture toughness (G_{IC}) tests are conducted using Double Cantilever Beam (DCB) specimen according to ASTM D5528-01 test standard. End notch flexure (ENF) test which is basically a 3-pt bending test is conducted in order to obtain Mode II (G_{IIC}) interlaminar fracture toughness. Curved beam strength is obtained by 4 point bending tests according to ASTM D6415/D6415M – 06a. Test set up pictures are given in the Figure 3. In the experiments Shimadzu Autograph AGS-J 10 kN screw driven tensile testing machine is used as the load indicator. In the DCB and ENF tests crack lengths are recorded by Canon 1D-X machine with Canon macro 100 mm lens during the experiments. During 4 point bending tests Photron SA5 high speed camera capable of maximum frame rate of 1,000,000 fps is used for recording delamination initiation and propagation. Specimens are loaded at 0.5 mm/min crosshead speed for all three type of tests. Load-displacement data is recorded digitally using Trapezedium software. Edge of the specimens are painted with the white paint to make the failure (crack) visible.

(a) (b) (c)

Figure 3. (a) DCB Test Setup, (b) ENF Test Setup, (c) 4 Point bending test Setup with high speed cameras.

3.1. DCB Test

In the DCB tests, when the initial crack becomes visible during loading the initial crack length, a_0, is verified. When the crack starts to propagate, load, P, and displacement, d, values are recorded and the actual crack length is measured. The peaks of the load-displacement curve are used as the load values in toughness calculations. This procedure is continued up to 45 mm crack growth to obtain fracture toughness resistance curves (R-curves). Mode-I fracture toughness is obtained by modified compliance calibration method according to ASTM D5528 [7] given by,

$$G_{IC} = \frac{3P^2C^{\frac{2}{3}}}{2A_1bh}, \tag{1}$$

where a is the initial crack length, P is the load, C is the compliance obtained by dividing the displacement by the load, b and h are width and thickness of the specimen, respectively, and A_1 is the slope of a/h versus $C^{1/3}$ curve.

3.2. ENF Test

Three point bending loading is applied on a precracked specimen in ENF tests. The test is unstable and stopped after the first load drop. Only one G_{IIC} value is obtained. Mode II fracture toughness is calculated based on direct beam theory [8] given by,

$$G_{IIC} = \frac{9a^2P\delta}{2b(2L^3 + 3a^3)}, \tag{2}$$

where δ is the load point deflection, L is the span length of the specimen.

3.3. Four Point bending test

Four point bending tests according to ASTM D6415/D6415M – 06a [9] are carried out in which pure moment is created at the corner. Load, P, and displacement, d, values are recorded when the delamination starts propagating in order to calculate the curved beam strength, CBS, and maximum radial stress, σ_r^{max}. Delamination propagation is recorded with high speed cameras. CBS and the approximate maximum radial stress are obtained from [9],

$$CBS = \frac{P}{2w\cos\varphi}\left(\frac{d_x}{\cos\varphi}\right) + (D + t)\tan\varphi), \tag{3}$$

$$\sigma_r^{max} = \frac{3CBS}{2t\sqrt{r_i r_o}}, \tag{4}$$

where φ is the angle of the arm of curved beam with the horizontal at failure, D is the diameter of the supports, t is the thickness of the specimen, d_x is the distance between lower and upper support, r_i and r_o are the inner and outer radii of the specimen corner, respectively.

4. Results

4.1. Mode-I Fracture Toughness test results

DCB test load-displacement curves for base and CNT added laminates are given in Figure 4. The load displacement behavior is similar for both types of specimens. Small sharp load drops and steady regions are observed for the base and CNT added specimens. Loading stiffness and the maximum load is higher for CNT added laminates. Corresponding R-curves for base and CNT added laminates are given in Figure 5a and 5b, respectively. R-curve of the base laminates (Figure 5a) is uniform and regular with low variation while the R-curve of CNT added laminates (figure 5b) has irregular rough behavior and scatter can be seen. Large scatter in the R-curve for CNT added laminates is attributed to the heterogeneous distribution of CNTs in the resin. Even if CNTs were well dispersed in the epoxy resin,

during resin covering in the manufacturing process CNTs might be repositioned and concentrated in clusters leading to heterogeneous distribution and property variation.

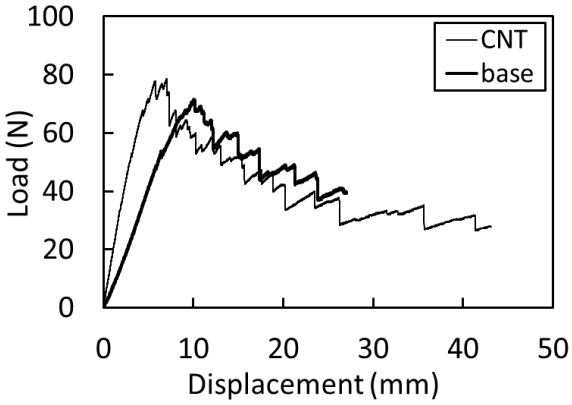

Figure 4. Load displacement curves of base and CNT added laminates from Mode I fracture toughness (DCB) test

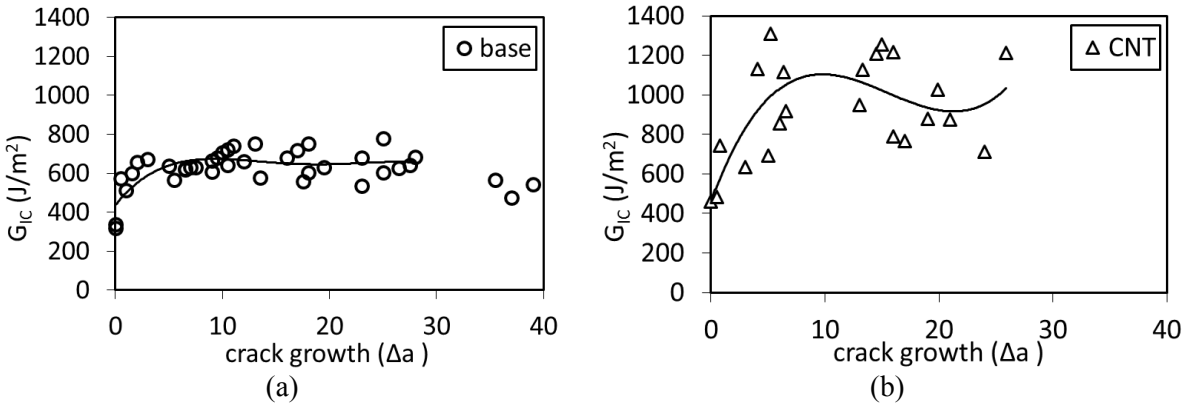

Figure 5. G_{Ic} Resistance curves for (a) base and (b) CNT added laminates

The bar graph of Mode I fracture toughness initiation ($G_{ICinitiation}$) and propagation ($G_{ICpropagation}$) values obtained by Equation 1 is given in Figure 6 below. An increase of 25% for Mode I fracture toughness initiation value and increase of 33% for the propagation value are observed with CNT addition. Scatter in $G_{ICpropagation}$ is found to be higher than the scatter in $G_{ICinitiation}$.

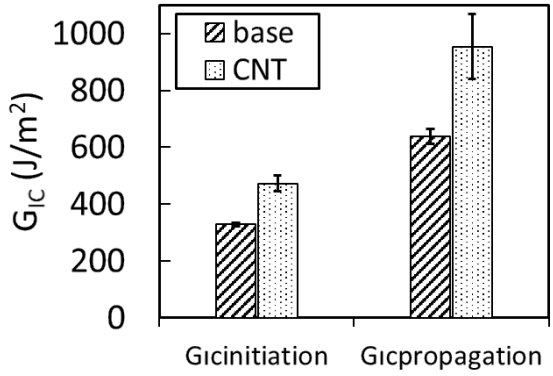

Figure 6. Mode I fracture toughness initiation and propagation values of base and CNT added laminates

In Figure 7a and 7b SEM images of fracture surfaces after DCB test is shown for base and CNT added laminates, respectively. Crack growth directions are shown by white arrows on the images. For the base laminate flat fracture surface is observed where the fabric layers are separated uniformly. In the CNT added laminate surface, holes are observed in the epoxy region and in some cases local regions of

fiber separation are observed. Thus, in the CNT added laminate, heterogeneity of delamination is observed which causes torturous crack path and increases the area of fracture contributing to increase in toughness.

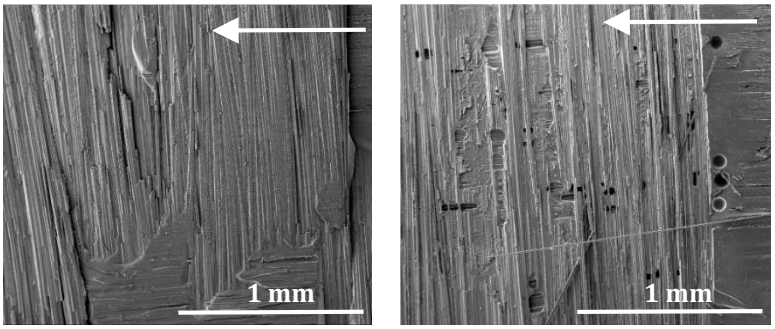

Figure 7. SEM images of fracture surfaces after DCB test for **(a)** base laminate, **(b)** CNT added laminate, arrow indicates the crack growth direction.

4.2. Mode-II fracture toughness test results

Load displacement curves for ENF tests of base and CNT added laminates are given in Figure 8a. Small stiffness change in between two materials is observed. For CNT added laminates sudden load drop after failure is observed in contrast to base materials in which load displacement stays irregular after failure. 3% wt CNT addition is found to increase maximum load at failure by approximately 20%. Bar graph of Mode II fracture toughness values of base and CNT added laminates obtained using Equation 2 are given in Figure 8b. 10% increase in Mode II fracture toughness is observed for CNT added laminates with much higher scatter in the Mode II toughness values as was also observed in DCB tests.

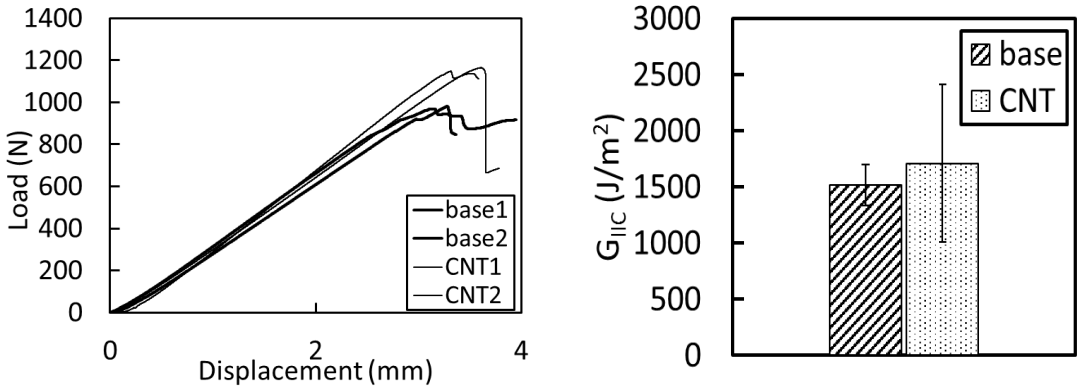

(a) (b)

Figure 8. (a) Load displacement curves for ENF test, (b) mode II fracture toughness results of base and CNT added laminates.

The large scatter and the increase in fracture toughness value for CNT added laminates can be attributed to scatter in the interface properties of the CNT specimens caused by the heterogeneous distribution of CNTs along the interface.

4.3. 4-Pt bending

Load-displacement curves of the 4-pt bending test for both the base material (thick line) and CNT added material (thin line) are shown in Figure 8. Results for two base materials and three CNT added materials are shown. In comparison with base material, stiffness is found to increase with CNT addition, however, the failure load is found to decrease with CNT addition. Base laminates can stand up to 2700 N and failure occurs at one load drop. In contrast to base material, two load drops are observed for the CNT added laminates. At the first load drop initial delamination occurs close to the upper edge of the specimen and it continues carrying load up to the second load drop without changing slope as will be discussed later. For CNT added laminates maximum load prior to failure is lower than the base material,

varying between 1500 and 1700 N. Scatter in the maximum load value of first and second load drop for the CNT added laminates supports the claim that non-uniform dispersion of CNTs during manufacturing might be leading to heterogeneous distribution and clumping of CNTs in the resin and property variation between different specimens.

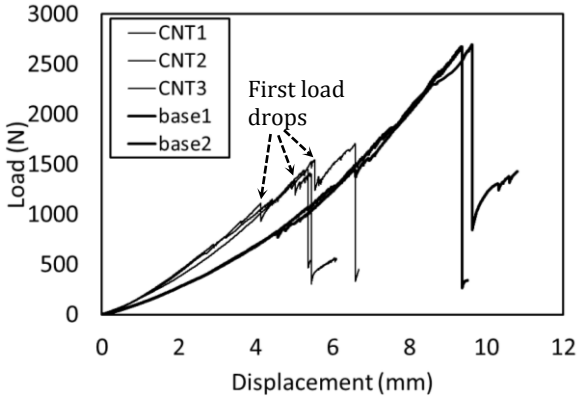

Figure 9. Load displacement curves of 4-pt bending test for base and CNT added laminates.

Curved beam strength (CBS) and maximum radial stress calculations are shown in Figures 10a and 10b, respectively. A 50% decrease in the CBS value and 64% percent decrease in the radial stress value occurs for the CNT added laminate. These results are in contrast to Avalon's study [1] where no effect of CNT addition on CBS and radial stress was observed. Mean value of curved beam strength of base laminate is about 800 N-mm/mm while CNT additions decreases the strength to 400 N-mm/mm. Large scatter for the CNT added material compared to the base material is also seen in 4-point rest results. Decrease in the maximum load decreases the strength and variation in maximum load leads to scatter in the results. These results also support the claim that reposition and concentration of CNTs in clusters with high density can lead to heterogeneities in the plies and non-isotropic mechanical properties that leads to variation and degradation in strength. In addition, decrease in the maximum radial stress is higher than CBS.

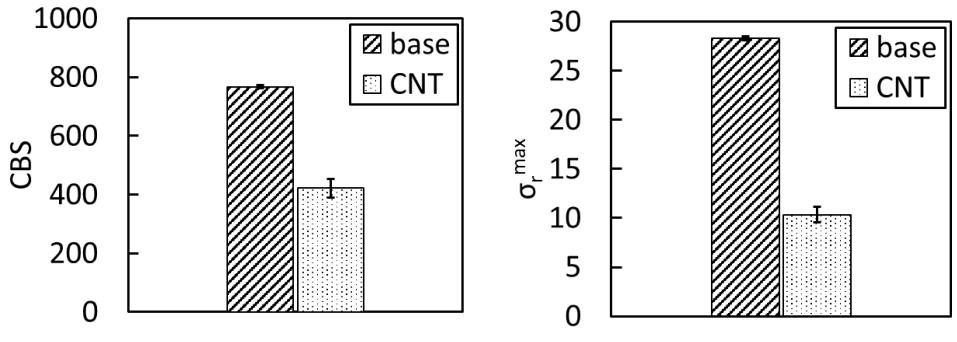

(a) (b)

Figure 10. (a) Curved beam strength, (b) maximum radial stress results of base and CNT added laminates

In order to see the delamination progression, digital image correlation was carried out at 7000 fps up to 1500N at each 20N load increment. DIC experiments were conducted with 25x25mm measuring volume in order to focus on the curved region in the specimen and visualize deformation field in detail. Since at high frame rates, the camera resolution is reduced to 256x185 pixels which are not sufficient to analyze strain variation in DIC system, high speed test and DIC test were conducted separately. In Figure 10, DIC images captured at 100N, 500N and 1500N are given. Epsilon-Y strain corresponding to opening stresses that lead to delamination are located close to the outer radius. According to the DIC results delamination nucleation is expected at the upper side of the curved region.

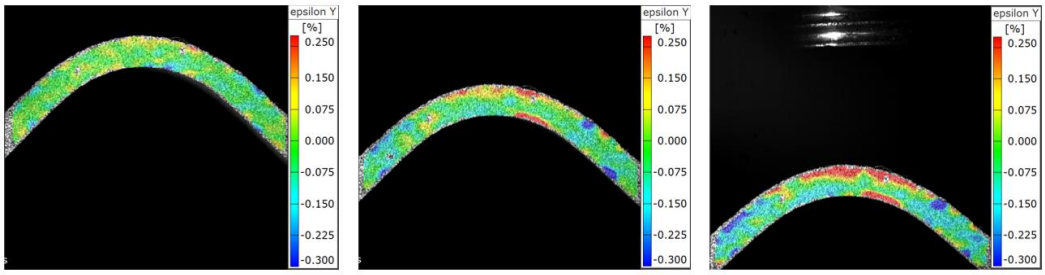

Figure 11. Full frame DIC images taken showing Epsilon-Y strain corresponding to opening stresses a) at 100N, b) at 500 N and c) at 1500N

High-speed camera image during delamination initiation and progression for base and CNT added specimens are given in Figures 12 and 13, respectively. For base laminates images were recorded at 15000 fps and for CNT specimens the images were recorded at 28000 fps. In Figure 12, nine sequential images taken at 0.66μs time interval show the failure sequence of base laminates recorded during the first load drop in which catastrophic failure occurs. The first delamination initiates close to the outer radius between 3rd and 4th plies. This result is consistent with the DIC results showing maximum opening strains close to the top surface (Fig. 11c). After the first delamination propagates to the arms from the center, 2nd delamination followed by a 3rd delamination occur sequentially from the outer radius to the inner radius with a spacing of 3 plies during this single load drop (Figure 8). Discontinuities can be observed in the delamination process due to the waviness of the interfaces in the plain weave fabric plies.

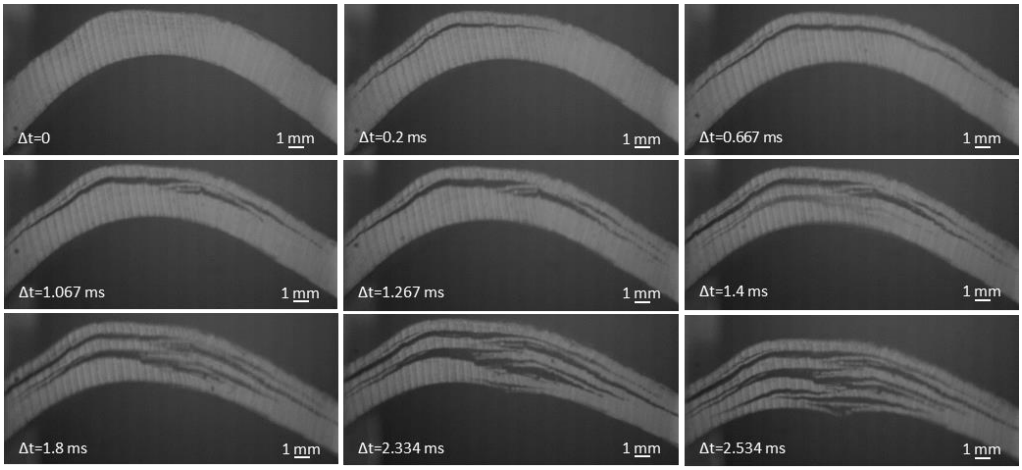

Figure 12. High speed camera images at 15,000 fps for base laminate.

The failure sequence is found to be different in the CNT added laminate that occurs at two different load drops. In Figures 13a and 13b, failure sequence of CNT added laminates at first and second load drop are given, respectively. At the first load drop a single delamination initiates close to the outer radius between 2nd and 3rd plies as in the base laminate and propagates slightly through both arms before arresting as seen in Figure 13a. After loading the material again, a second load drop is observed in which further delamination sequence is shown in Figure 13b. During this load drop, initial delamination continues to propagate and a second crack initiates at the last ply and propagates diagonally between different laminates. Third crack occurs above the second crack close to mid layer. Fourth crack initiates between first and third delamination and kinking can be clearly seen. However, between the major cracks, secondary cracks tend to mender to the weak CNT clustered regions changing the interlaminar crack paths. No merging cracks or fiber bridging is observed and total delamination sizes are smaller compared to base laminates possibly due to arresting of cracks in the corner region by the CNT clusters.

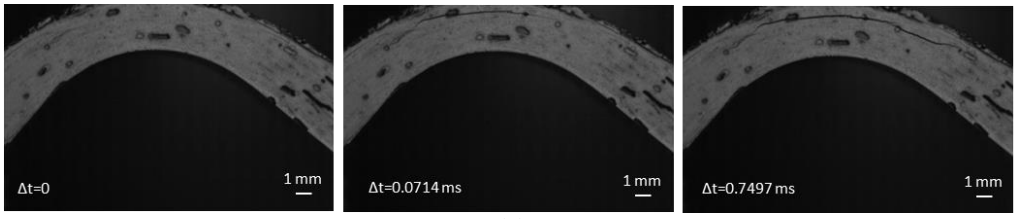

(a)

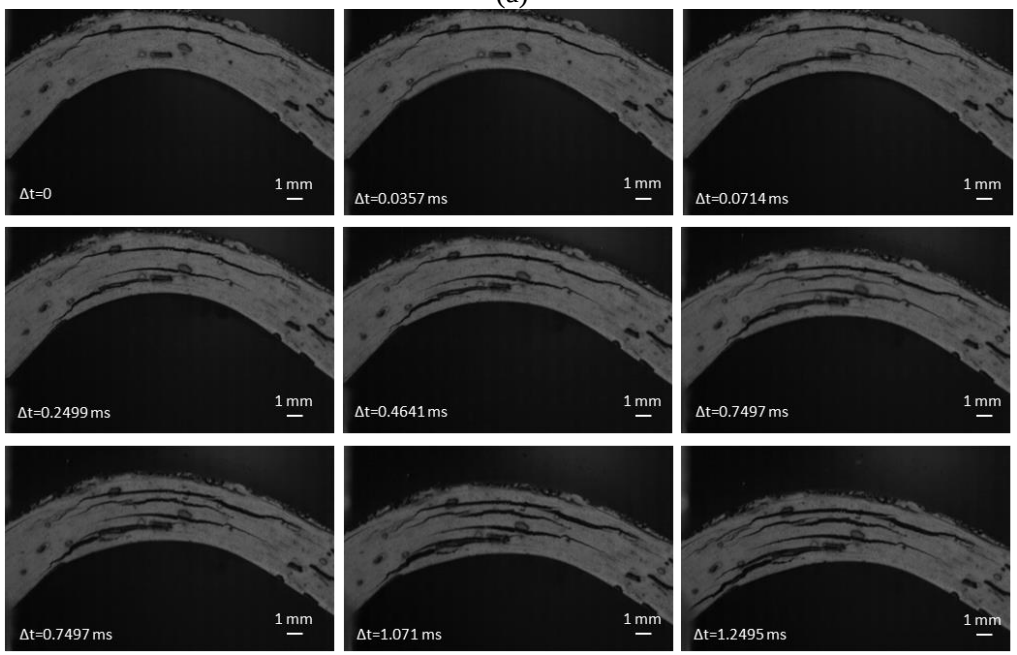

(b)

Figure 13. High speed camera images at 28,000 fps for CNT added laminate at (a) first load drop and (b) second load drop.

5. Conclusions

In this study change in the Mode I, Mode II fracture toughness and curved beam strength of carbon/epoxy fabric laminates with 3% wt CNT addition in the resin was investigated by conducting DCB, ENF and 4 point bending tests, respectively. CNT dispersion in the resin was provided by mixing high fraction (20%) CNT added Epocyl^{TM} NCR128-02 liquid Bisphenol-A epoxy resin with Araldite® LY 5052 epoxy resin then covering the fabrics.

- Mode I initiation fracture toughness is increased by %25 and mode II fracture toughness is increased by %10 compared to base laminates.
- Curved beam strength decreased by 50% percent and the radial stress decreased 64% percent decrease for the CNT added laminate. Higher scatter was seen in all tests for the CNT added laminates compared to the base specimens. This result is attributed to heterogeneity and local concentration of CNTs resulting in property variation between different specimens.
- Maximum opening stress location was found to be close to the outer radius from the DIC images and failure was expected at this location for the base material. High speed camera images showed that first delamination initiated and propagated close to the outer radius where maximum opening stresses located.
- With the 3% wt CNT addition, change of failure sequence from one load drop to two load drops was observed. Initial delamination close to the upper edge at the first load drop and failure with multiple delaminations at the second load drop was observed.

Acknowledgments
This work was supported by the Ministry of Science, Industry and Technology and Turkish Aerospace Industries and the research was conducted in the METU Center for Wind Energy. The authors would also like to acknowledge the contribution of Denizhan Yavas in the experiments.

6. References

[1] Avalon S C and Donalson S L, "Strength of composite angle brackets with multiple geometries and nanofiber-enhanced resins," Journal of Composite Materials, vol. 45(9), pp. 1017-1030, 2010.
[2] Hao W, Ge D, Ma Y, Yao X and Shi Y, "Experimental investigation on deformation and strength of carbon/epoxy," Polymer Testing, vol. 31, pp. 520-526, 2012.
[3] Seyhan A T, Tanoglu M and Schulte K, "Mode I and mode II fracture toughness of E-glass non-crimp fabric/carbon nanotube (CNT) modified polymer based composites," Engineering Fracture Mechanics, no. 75, pp. 5151-5162, 2008.
[4] Godara A, Mezzo L, Luizi F, Warrier A, Lomov S V, van Vuure A W, Gorbatikh L, Mondenaers P and Verpoest I, "Influence of carbon nanotube reinforcement on the processing and the mechanical behaviour of carbon fiber/epoxy composites," C A R B ON, no. 47, pp. 2914-2923, 2009.
[5] E. J. Garcia, B. L. Wardle and A. J. Hart, "Joining prepreg composite interfaces with aligned carbon nanotubes," Composites: Part A, no. 39, p. 1065–1070, 2008.
[6] M. Arai, Y. Noro, K. Sugimoto and M. Endo, "Mode I and Mode II interlaminar fracture toughness of CRFP laminates by carbon nanofiber interlayer," Composites Science and Technology, pp. 68: 516-552, 2008.
[7] ASTM D5528-01, Standard Test Method for Mode I Interlaminar Fracture Toughness of Unidirectional Fiber-Reinforced Polymer Matrix Composites, West Conshohocken, PA, 19428 USA: ASTM International 2007.
[8] Russel A.J., "On the Measurement of Mode II Interlaminar Energies", Defense Research Establishment Pacific, Materials Report-82., Department of National Defense, Canada, 1982.
[9] ASTM D6415/D6415M – 06a, Standard Test Method for Measuring the Curved Beam Strength of a Fiber-Reinforced Polymer-Matrix Composite, West Conshohocken, PA,19428 USA: ASTM International 2007.